

**Thermal boundary resistance at Au/Ge/Ge and Au/Si/Ge interfaces**

Journal:	<i>RSC Advances</i>
Manuscript ID:	RA-ART-03-2015-004412.R1
Article Type:	Paper
Date Submitted by the Author:	20-May-2015
Complete List of Authors:	ZHAN, TIANZHUO; National Institute for Materials Science, Xu, Yibin; National Institute for Materials Science, Goto, Masahiro; National Institute for Materials Science, MANA Nano-Electronics Materials Unit Tanaka, Yoshihisa; National Institute for Materials Science, Kato, Ryoza; National Institute for Materials Science, Sasaki, Michiko; National Institute for Materials Science,

ARTICLE

Thermal boundary resistance at Au/Ge/Ge and Au/Si/Ge interfaces

Cite this: DOI: 10.1039/x0xx00000x

T. Zhan*, Y. Xu, M. Goto, Y. Tanaka, R. Kato and M. Sasaki

Received 00th January 2012,
Accepted 00th January 2012

DOI: 10.1039/x0xx00000x

www.rsc.org/

Amorphous Ge (a-Ge), crystalline Ge (c-Ge), and amorphous Si (a-Si) thin films were deposited on a Ge substrate at different temperatures by magnetron sputtering. We measured thermal boundary resistance (TBR) in Au/Ge/Ge and Au/Si/Ge three-layer samples. The measured TBR in Au/a-Ge/Ge and Au/a-Si/Ge decreased slightly with increasing deposition temperature. The measured TBR values were larger than the values predicted by the diffuse mismatch model. Furthermore, it is interesting to note that the measured TBR in Au/c-Ge/Ge was twofold larger than that in Au/a-Ge/Ge. Cross-sectional transmission electron microscopy was conducted to investigate interfacial morphology of the samples. The results indicate that the crystalline state of the deposited thin films play an important role in TBR by modifying phonon density of states and interfacial properties. Our findings are of great importance for applications involving thermal management of micro- and optoelectronic devices, and for the development of thermal barrier coatings and thermoelectric materials with high figures-of-merit.

1. Introduction

Thermal boundary resistance (TBR) is defined as the ratio of the temperature discontinuity at an interface to the heat flux flowing across that interface.¹ Typically, the overall thermal resistance of a material system comprises the thermal resistance of the constituent materials and the TBR between those materials. However, in nanoscale semiconductor systems, the characteristic length scales, which may be shorter than the phonon mean free paths (MFPs), lead to phonon transport in these materials being ballistic rather than diffusive. Moreover, the spatial density of the interfaces increases with the decreasing length scale in nanoscale material systems. Thus, the TBR dominates the overall thermal resistance.² The investigation of TBR is vital for applications involving thermal management of micro- and optoelectronic devices (e.g., Schottky barriers and ohmic contacts)³, and for the development of thermal barrier coatings⁴ and thermoelectric materials with high figures-of-merit.^{5,6}

Several theoretical methods have been developed to predict TBR. The acoustic mismatch model (AMM)⁷ and the diffuse mismatch model (DMM)¹ are typically used for predicting the TBR. In AMM and DMM, the transmission probability of the phonons at interfaces is related to the acoustic impedances and phonon density of states (DOS) of the Debye model on both sides of the interface, respectively. However, in the two models, the effects of interfacial properties, such as roughness and diffusion, on TBR are not taken into account. Thus,

molecular dynamics⁸⁻¹⁰ has been used to predict TBR. The effects of interfacial properties on TBR have been investigated in a number of theoretical studies.¹¹⁻¹⁷ However, the effects have been experimentally investigated only recently.¹⁸⁻²⁵ For example, the mixing layer thickness and compositional change due to diffusion were found to affect the TBR at the Cr/Si interface.¹⁸ Also, it was found that TBR increases with increasing Si surface roughness at the Al/Si interface.²⁰ Another recent finding is that interfacial roughness has a negligible effect on TBR at the Au/Si interface.²³ However, the experimental data are too limited to understand the effects of interfacial properties on TBR.

In this study, we prepared two series of three-layer samples consisting of two interfaces (Au/Ge/Ge and Au/Si/Ge) by magnetron sputtering. Amorphous Ge (a-Ge), crystalline Ge (c-Ge), and amorphous Si (a-Si) thin films were deposited on single-crystalline Ge substrates at different temperatures. We measured TBR at two interfaces in Au/Ge/Ge and Au/Si/Ge samples. We found that TBR in Au/a-Ge/Ge and Au/a-Si/Ge decreased slightly with increasing deposition temperature. The measured TBR values were larger than the values predicted by the DMM. The measured TBR was significantly larger in Au/c-Ge/Ge than in Au/a-Ge/Ge. We characterized the interfacial morphology of the samples by cross-sectional high-resolution transmission electron microscopy (HRTEM) to investigate the mechanisms underlying the difference in the measured TBR.

2. Experimental

We prepared the samples by magnetron sputtering with a laboratory-built combinatorial sputtering system. For one series, Ge thin films were deposited on single-crystalline Ge substrates at 25, 300, and 500 °C. For the other series, Si thin films were deposited on single-crystalline Ge substrates at 25, 300, and 500 °C. The sputtering power was 100 W. An Au film was deposited on the Ge and Si thin films to form Au/Ge and Au/Si interfaces. The Au film also serves as a laser absorber and temperature sensor. The Au films were deposited at 25 °C. The single-crystalline Ge substrates were 0.5 mm thick. The target thicknesses were 15 nm for the Ge and Si thin films, 150 nm for the Au films.

The TBR of the samples was measured by the ω method²⁶ at 25 °C under vacuum (<0.02 Pa). The Au film was heated by a pump laser (405 nm) with angular frequency ω . The temperature at the Au film surface was detected by a probe laser (635 nm) by the thermoreflectance technique. Using the one-dimensional heat conduction equation for the sample system,^{27,28} we can obtain the temperature at the surface of the Au film, $T(0)$:

$$\frac{T(0)}{qd_0} = \frac{e^{-\frac{\pi}{4}}}{\sqrt{2\omega\lambda_2 C_2}} + R_{01} + R_{12} + \left(1 - \frac{\lambda_1 C_1}{\lambda_2 C_2}\right) \frac{d_1}{\lambda_1} + \left(1 - \frac{\lambda_0 C_0}{\lambda_2 C_2}\right) \frac{d_0}{\lambda_0} \quad (1)$$

Here, d is the film thickness, q is the heat flux, λ is the thermal conductivity, and C is the volumetric heat capacity. Subscripts 0, 1, and 2 denote the Au film, the middle layer, and the substrate, respectively. R_{01} and R_{12} are the TBR at the Au/middle layer and middle layer/substrate interfaces, respectively. The fourth and fifth terms on the right-hand side of Eq. (1) are the thermal resistance of the middle layer and Au film, respectively. The measurements were carried out at frequencies from 4 to 32 kHz. A linear plot of $(T(0))/(qd_0)$ versus $1/\sqrt{\omega}$ was obtained, in which the intercept R at $1/\sqrt{\omega} = 0$ corresponds to the sum of the second, third, fourth, and fifth terms on the right-hand side of Eq. (1). Thermal resistance was measured at three different locations on each sample, and each measurement was performed in triplicate to reduce the error. The interface morphology of the samples was characterized by cross-sectional HRTEM (9000NAR, Hitachi Corp.).

3. Results and discussion

Figure 1(a)–(d) shows the cross-sectional HRTEM images of the interfacial morphology of the Au/Ge/Ge samples prepared at 25, 300, and 500 °C, and the Au/Si/Ge sample prepared at 25 °C, respectively. The Ge thin films deposited at 25 and 300 °C, and the Si thin film deposited at 25 °C showed no evidence of crystallinity, whereas the Ge thin film deposited at 500 °C showed a crystalline structure. The crystalline state of the Ge and Si thin films was also confirmed by X-ray diffraction in our previous study.²⁹ Furthermore, the interfaces between the Au film and the middle layer showed different morphology. The Au/a-Ge and Au/a-Si interfaces were rough, whereas the Au/c-Ge interface was relative smooth. The

thickness of the deposited a-Ge and a-Si thin films was different from the target thickness. The a-Ge and a-Si thin films had an average thickness of 10 and 25 nm, respectively, and the c-Ge thin film was 15 nm thick.

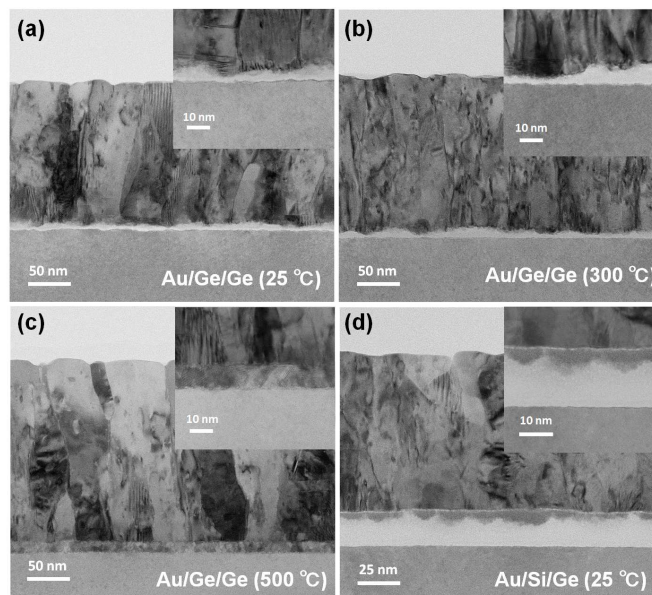


Figure 1. Cross-sectional HRTEM images of the interface morphology in Au/Ge/Ge and Au/Si/Ge samples prepared at different temperatures. The insets show higher-resolution images of the interface morphology.

The measured total thermal resistance (intercept R) consists of four parts: TBR at the Au/middle layer interface, TBR at the middle layer/substrate interface, thermal resistance of the middle layer, and thermal resistance of the Au film. To determine the TBR at the two interfaces, the thermal resistance of the middle layer and Au film should be subtracted from the total thermal resistance. We have measured the thermal conductivity of the Ge and Si thin films deposited at 25, 300, and 500 °C in our previous study.²⁹ The thermal conductivities of the Ge thin films (100 nm thick) deposited at 25, 300, and 500 °C were 1.00, 1.15, and 5.68 W/(m·K), respectively. The thermal conductivities of the Ge thin films in this study should be lower than these values owing to the thickness dependence.²⁹ Using these values, we estimated the thermal resistance of the Ge thin films deposited at 25, 300, and 500 °C to be 10, 8.7, and 2.6×10^{-9} m²·K/W, respectively. Thus, the TBR at two interfaces in the Au/Ge/Ge samples prepared at 25, 300, and 500 °C were 15.8, 15.3, and 33.6×10^{-9} m²·K/W, respectively. For the Au/Si/Ge samples, the measured thermal conductivities of the Si thin films (100 nm thick) deposited at 25, 300, and 500 °C were 0.93, 0.94, and 0.98 W/(m·K), respectively.²⁹ We estimate the thermal resistance of the Si thin films deposited at 25, 300, and 500 °C to be 26.9, 26.6, and 25.5×10^{-9} m²·K/W. Thus, the TBR at two interfaces in the Au/Si/Ge samples prepared at 25, 300, and 500 °C were 25, 22.6, and 20.7×10^{-9} m²·K/W, respectively.

Figure 2 shows the measured TBR at two interfaces as a function of the deposition temperature for the two series of samples. The DMM-predicted values were also plotted for comparison. For both Au/a-Ge/Ge and Au/a-Si/Ge samples, the TBR at two interfaces decreased slightly with increasing deposition temperature. All the measured TBR values were larger than the DMM-predicted values. Furthermore, it is noteworthy that the TBR at the two interfaces in the Au/c-Ge/Ge samples were twofold larger than that in the Au/a-Ge/Ge samples. We next discuss the possible mechanisms for the difference in the TBR between the different samples.

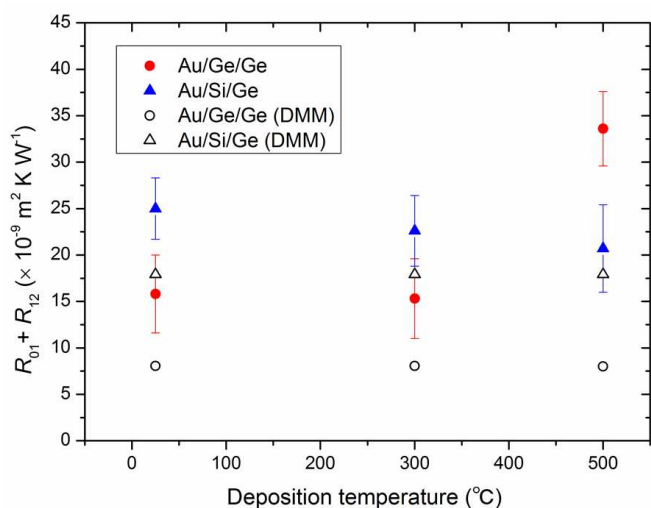


Figure 2. Measured TBR at two interfaces in Au/Ge/Ge and Au/Si/Ge three-layer samples as a function of deposition temperature. DMM-predicted values are plotted for comparison.

In our previous study, we showed that the thermal conductivity of the a-Si and a-Ge thin films prepared by magnetron sputtering decreased with increasing deposition temperature. We attributed the difference in the thermal conductivity to the modification of the microstructure in a-Si and a-Ge thin films as the deposition temperature was increased.^{29,30} In this study, the TBR at two interfaces in the Au/a-Ge/Ge and Au/a-Si/Ge samples decreased slightly with increasing deposition temperature, which showed similar dependence to the thermal conductivity of a-Si and a-Ge thin films. We also attributed this dependence to the modification of the microstructure in a-Si and a-Ge thin films. We suggest that the change of phonon group velocity, phonon MFPs, and phonon DOS due to the modification of the microstructure may cause this dependence. However, the density and phonon group velocity in the thin films should not change greatly with increasing deposition temperature due to the totally amorphous nature of the thin films. This indicates that the effects of phonon group velocity and phonon DOS on the decrease of the measured TBR can be neglected. Furthermore, based on the minimum thermal conductivity model, the phonon MFPs in a-Si and a-Ge are extremely short, which are on the order of the interatomic spacing of Si and Ge, respectively. This indicates that phonon MFPs in these amorphous thin films should be the

same. However, in our previous studies, we have shown that phonons with MFPs longer than 100 nm contribute to heat transport in a-Si and a-Ge. Furthermore, as deposition temperature was increased, phonons with MFPs identical with film thickness increased with increasing deposition temperature in a-Si and a-Ge thin films.²⁹ The increase of such long MFPs phonons may facilitate heat transport across the interface and cause the decrease of TBR as deposition temperature was increased. However, we do not yet understand how long MFPs phonons facilitate heat transport across the interface, which needs further investigation.

In Figure 2, for both Au/a-Ge/Ge and Au/a-Si/Ge samples, the DMM underestimated the TBR at two interfaces. However, the difference in the measured TBR between the two series samples was similar to that in the DMM-predicted values. The TBR for Au/c-Ge/Ge was also predicted by the DMM ($8.01 \times 10^{-9} \text{ m}^2 \cdot \text{K/W}$), which was significantly lower than the measured TBR. In the DMM, the TBR is dependent on the phonon DOS of the Debye model on both sides of the interface. In this study, the exact phonon DOS in the Si and Ge thin films should be different from the phonon DOS of the Debye model, resulting in the difference between the measured TBR and the DMM-predicted values. In addition, in the DMM, the effects of the interface properties on TBR are not taken into account. Thus, the interfacial properties of the Au/Ge and Au/Si interfaces, such as interfacial structural disorder and diffusion, may decrease the transmission probability of phonons at the interface, resulting in a measured TBR larger than the DMM-predicted values. The large discrepancy in the measured TBR and DMM-predicted values in Au/c-Ge/Ge sample further indicated that interfacial properties played an important role in TBR in addition to the mismatch in phonon DOS on both sides of the interface.

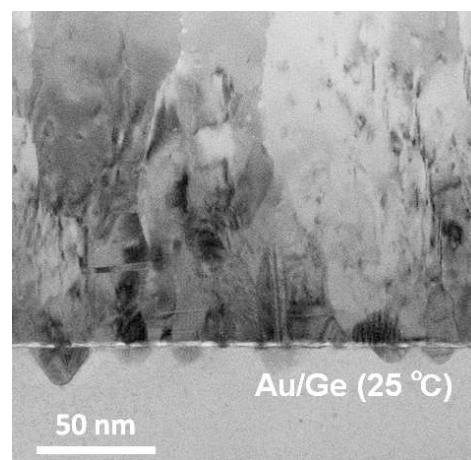


Figure 3. Cross-sectional HRTEM images of the interface morphology in the Au/c-Ge sample prepared at 25 °C.

The DMM predicted almost the same TBR at two interfaces in Au/a-Ge/Ge ($8.05 \times 10^{-9} \text{ m}^2 \cdot \text{K/W}$) and Au/c-Ge/Ge ($8.01 \times 10^{-9} \text{ m}^2 \cdot \text{K/W}$). However, it is interesting to note that the measured TBR at the two interfaces in Au/c-Ge/Ge ($33.6 \times 10^{-9} \text{ m}^2 \cdot \text{K/W}$) was twofold larger than that in Au/a-Ge/Ge ($15.8 \times$

$10^{-9} \text{ m}^2 \cdot \text{K/W}$). We speculate that the large measured TBR at the two interfaces in Au/c-Ge/Ge mainly come from the Au/Ge interface rather than the Ge/Ge interface. To verify our speculation, we performed additional experiments to rule out the effect of the Ge/Ge interface. We deposited an Au film directly on a single-crystalline Ge substrate at 25 °C and measured the TBR at the Au/c-Ge interface. The measured TBR was $29.8 \pm 3.8 \times 10^{-9} \text{ m}^2 \cdot \text{K/W}$ (not shown in Figure 2), which was slightly smaller than the TBR at two interfaces in Au/c-Ge/Ge samples prepared at 500 °C. The results indicate that the Au/c-Ge interface contributed the most to the TBR in the Au/c-Ge/Ge sample, and the TBR at the c-Ge/Ge interface was only $3.8 \times 10^{-9} \text{ m}^2 \cdot \text{K/W}$. We attribute the twofold difference in TBR between Au/c-Ge/Ge and Au/a-Ge/Ge to the different crystalline state of the deposited Ge thin films. As the deposition temperature was increased from 25 to 500 °C, the Ge thin film began to crystallize, causing the modification of the density and phonon group velocity in the Ge thin films. The modification of the density and phonon group velocity would change the Debye temperature of Ge. The Debye temperatures of Au, a-Ge, and c-Ge are estimated to be 170, 190, and 322 K, respectively. This indicates that the mismatch in phonon DOS between Au and Ge enhanced as the Ge thin film crystallized. The enhancement of the mismatch in phonon DOS would increase the TBR. On the other hand, the phonon group velocity in c-Ge ($3.46 \times 10^3 \text{ m/s}$) are larger than that in a-Ge ($2.86 \times 10^3 \text{ m/s}$). The increase of phonon group velocity would decrease the TBR by increasing the heat flux flowing across the interfaces. Furthermore, the phonon MFPs also increased as the Ge thin film crystallized, which would decrease the TBR as well. That is to say, the effects of phonon group velocity and phonon MFPs counteracted the effects of the enhancement of mismatch in phonon DOS on increasing TBR. We suggest that only the enhancement of mismatch in phonon DOS should not lead to the twofold difference in the measured TBR between Au/a-Ge/Ge and Au/c-Ge/Ge samples; some interfacial properties also play an important role in increasing TBR. The modification of interfacial properties due to the different crystalline state of the thin films may change the inelastic scattering rate of phonons, increasing the TBR. In order to further understand the difference in interfacial properties between Au/c-Ge and Au/a-Ge interfaces, we also conducted cross-sectional HRTEM to investigate the interfacial morphology at the Au/c-Ge interface. Figure 3 showed that the Au/c-Ge interface was smooth, which was different from the rough Au/a-Ge interfaces in Au/a-Ge/Ge samples prepared at 25 and 300 °C. Furthermore, crater-shaped diffusion between the Au and the single-crystalline Ge substrate is clearly visible in Figure 3. Au has different diffusion mechanisms in c-Ge and a-Ge, and thus Au has a higher diffusion coefficient in a-Ge than in Au/c-Ge^{31, 32}. Thus, we believe that diffusion at the Au/a-Ge interface also occurred. The different mixing layers formed by Au/a-Ge and Au/c-Ge diffusion may also affect the phonon transmission probability at the interface. However, we do not yet understand how the interfacial diffusion affected TBR. We can only speculate that the diffusion at Au/c-Ge

interface together with other interfacial properties increased the TBR comparing with the case of Au/a-Ge. The combined effects of the phonon group velocity, phonon MFPs, the enhancement of mismatch in phonon DOS and interfacial properties due to the different crystalline state of the deposited thin films caused the twofold difference in the measured TBR between the Au/a-Ge/Ge and Au/c-Ge/Ge samples.

Many theoretical studies have been performed to investigate the effects of heat flow direction, film thickness, and period length on TBR in superlattice systems, and also the effects of interfacial properties, such as interfacial mixing, structural disorder, dislocation, roughness, and bonding strength on TBR.³³⁻⁴² However, the investigation of the effects of crystalline state of thin films on TBR were limited. In this study we showed that the crystalline state of thin films could affect TBR significantly. Our findings provide new information for the future theoretical and experimental studies on TBR.

Conclusions

In summary, we measured TBR at two interfaces in Au/Ge/Ge and Au/Si/Ge three-layer samples. We found that TBR in Au/a-Ge/Ge and Au/a-Si/Ge decreased slightly with increasing deposition temperature. All the measured TBR were larger than the DMM-predicted values. Furthermore, the measured TBR was twofold larger in Au/c-Ge/Ge than in Au/a-Ge/Ge. Cross-sectional HRTEM was conducted to investigate the mechanisms underlying these results. The results indicate that the modification of the microstructure in a-Si and a-Ge thin film increased the phonons with MFPs identical with film thickness, causing the deposition temperature dependence of the measured TBR. The change of the crystalline states of the deposited Ge thin films modified the phonon DOS and interfacial properties, causing the twofold difference in the measured TBR in Au/a-Ge/Ge and Au/c-Ge/Ge samples. Our findings are of great importance for applications involving thermal management of micro- and optoelectronic devices, and for the development of thermoelectric materials with high figures-of-merit.

Acknowledgements

This work was supported by MEXT KAKENHI Grant Number 23560813.

Notes and references

National Institute for Materials Science, 1-2-1 Sengen, Tsukuba 305-0047, Japan, *Electronic mail: ZHAN.Tianzhuo@nims.go.jp.

- 1 E.T. Swartz and R. O. Pohl, *Rev. Mod. Phys.*, **1989**, *61*, 605-668.
- 2 D. G. Cahill, W. K. Ford, K. E. Goodson, G. D. Mahan, A. Majumdar, H. J. Maris, R. Merlin, and S. R. Phillpot, *J. Appl. Phys.*, **2003**, *93*, 793-818
- 3 S. M. Sze, *Physics of Semiconductor Devices*, 2nd ed. Wiley, New York, 1981.
- 4 N. P. Padture, M. Gell, and E. H. Jordan, *Science*, **2002**, *296*, 280-284

- 5 G. Chen, *Phys. Rev. B*, **1998**, *57*, 14958-14973.
- 6 R. Venkatasubramanian, E. Siivola, T. Colpitts, and B. O'Quinn, *Nature*, **2013**, *413*, 597-602.
- 7 W. A. Little, *Can. J. Phys.*, **1959**, *37*, 334-349.
- 8 S. Volz, J. Saulnier, G. Chen, and P. Beauchamp, *Microelectron. J.*, **2000**, *31*, 815-819.
- 9 P. K. Schelling, S. R. Phillpot, and P. Keblinski, *Phys. Rev. B*, **2002**, *65*, 144306.
- 10 R. J. Stevens, L. V. Zhigilei, and P. M. Norris, *Int. J. Heat Mass Transfer*, **2007**, *50*, 3977-3989.
- 11 T. E. Beechem, S. Graham, P. E. Hopkins, and P. M. Norris, *Appl. Phys. Lett.*, **2007**, *90*, 054104.
- 12 D. Kechrakos, *J. Phys.: Condens. Matter*, **1990**, *2*, 2637-2652.
- 13 A. G. Kozorezov, J. K. Wigmore, C. Erd, A. Peacock, and A. Poelaert, *Phys. Rev. B*, **1998**, *57*, 7411-7414.
- 14 R. S. Prasher and P. E. Phelan, *J. Heat Transfer*, **2001**, *123*, 105-112.
- 15 S.-F. Ren, W. Cheng, and G. Chen, *J. Appl. Phys.*, **2006**, *100*, 103505.
- 16 J.-Y. Duquesne, *Phys. Rev. B*, **2009**, *79*, 153304.
- 17 M. Hu, P. Keblinski, and P. K. Schelling, *Phys. Rev. B*, **2009**, *79*, 104305.
- 18 P. E. Hopkins and P. M. Norris, *Appl. Phys. Lett.*, **2006**, *89*, 131909.
- 19 P. E. Hopkins and P. M. Norris, R. J. Stevens, T. E. Beechem, and S. Graham, *J. Heat Transfer*, **2008**, *130*, 062402.
- 20 P. E. Hopkins, L. M. Phinney, J. R. Serrano, and T. E. Beechem, *Phys. Rev. B*, **2010**, *82*, 085307.
- 21 P. E. Hopkins, J. C. Duda, C. W. Petz, and J. A. Floro, *Phys. Rev. B*, **2011**, *84*, 035438.
- 22 J. C. Duda and P. E. Hopkins, *Appl. Phys. Lett.*, **2012**, *100*, 111602.
- 23 J. C. Duda, C.-Y. P. Yang, B. M. Foley, R. Cheaito, D. L. Medlin, R. E. Jones, and P. E. Hopkins, *Appl. Phys. Lett.*, **2013**, *102*, 081902.
- 24 P. J. O'Brien, S. Shenogin, J. Liu, P. K. Chow, D. Laurencin, P. H. Mutin, M. Yamaguchi, P. Keblinski and G. Ramanath, *Nat. Mat.*, **2013**, *12*, 118-122.
- 25 B. Gotsmann and M. A. Lantz, *Nat. Mat.*, **2013**, *12*, 59-65.
- 26 R. Kato, Y. Xu, and M. Goto, *Jpn. J. Appl. Phys.*, **2011**, *50*, 106602.
- 27 Y. Xu, R. Kato and M. Goto, *J. Appl. Phys.*, **2010**, *108*, 104317.
- 28 Y. Xu, M. Goto, R. Kato, Y. Tanaka, and Y. Kagawa, *J. Appl. Phys.*, **2012**, *111*, 084320.
- 29 T. Z. Zhan, Y. Xu, M. Goto, Y. Tanaka, R. Kato, M. Sasaki, and Y. Kagawa, *Appl. Phys. Lett.*, **2014**, *104*, 071911.
- 30 T. Z. Zhan, Y. Xu, M. Goto, Y. Tanaka, R. Kato, M. Sasaki, and Y. Kagawa, *AIP Adv.*, **2014**, *4*, 027126.
- 31 S. Coffa, J. M. Poate, D. C. Jacobson, W. Frank, and W. Gustin, *Phys. Rev. B*, **1992**, *45*, 8355-8358.
- 32 W. Frank, *Defect and Diffusion Forum*, **1997**, *695*, 143-147.
- 33 S. R. Phillpot, P. K. Schelling, and P. Keblinski, *J. Mat. Sci.*, **2005**, *40*, 3143-3148.
- 34 T. Z. Zhan, S. Minamoto, Y. Xu, Y. Tanaka, and Y. Kagawa, *AIP Adv.*, **2015**, *5*, 047102.
- 35 H. Zhong and J. R. Lukes, *Phys. Rev. B*, **2006**, *72*, 174302.
- 36 E. S. Landry and A. J. H. McGaughey, *Phys. Rev. B*, **2009**, *80*, 165304.
- 37 E. S. Landry and A. J. H. McGaughey, *Phys. Rev. B*, **2009**, *79*, 075316.
- 38 V. Samvedi and V. Tomar, *Nanotechnology*, **2009**, *20*, 365701.
- 39 V. Samvedi and V. Tomar, *J. Appl. Phys.*, **2009**, *105*, 013541.
- 40 V. Samvedi and V. Tomar, *J. Appl. Phys.*, **2013**, *114*, 034312.
- 41 X. Li, and R. Yang, *Phys. Rev. B*, **2012**, *86*, 054305.